Integrin-Mediated Targeted Cancer Therapy Using c(RGDyK)-Based Conjugates of Gemcitabine

Theodora Chatzisideri, George Leonidis, Theodoros Karampelas, Eleni Skavatsou, Angeliki Velentza-Almpani, Francesca Bianchini, Constantin Tamvakopoulos,* and Vasiliki Sarli*

Cite This: *J. Med. Chem.* 2022, 65, 271−284

Read Online

ACCESS | 📊 Metrics & More | 📰 Article Recommendations | 🆘 Supporting Information

ABSTRACT: c(RGDyK)-based conjugates of gemcitabine (GEM) with the carbonate and carbamate linkages in the 6-OH group of GEM were synthesized for the targeted delivery of GEM to integrin $\alpha_v\beta_3$, overexpressing cancer cells to increase the stability as well as the tumor delivery of GEM and minimize common side effects associated with GEM treatment. Competitive cell uptake experiments demonstrated that conjugate **TC113** could be internalized by A549 cells through integrin $\alpha_v\beta_3$. Among the synthesized conjugates, **TC113** bearing the carbamate linker was stable in human plasma and was further assessed in an *in vivo* pharmacokinetic study. **TC113** appeared to be relatively stable, releasing GEM slowly into blood, while it showed potent antiproliferative properties against WM266.4 and A549 cells. The encouraging data presented in this study with respect to **TC113** provide a promising keystone for further investigation of this GEM conjugate with potential future clinical applications.
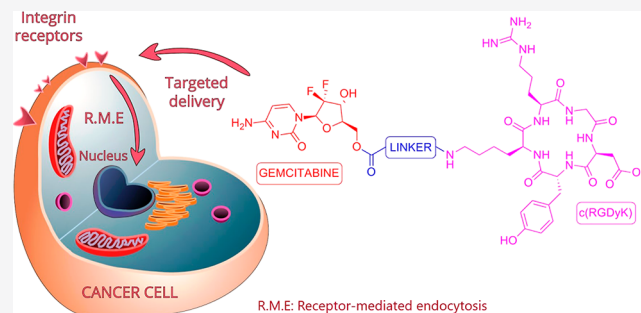
INTRODUCTION

Gemcitabine (GEM, also known as Gemzar) is a pyrimidine nucleoside antimetabolite drug used as monotherapy or in combination with chemotherapeutic agents or radiotherapy[1] to treat pancreatic,[2] ovarian, breast,[3] and non-small-cell lung cancers.[4] The uptake mechanisms of GEM include nucleoside transporter (NT) proteins such as human equilibrative nucleoside transporter 1 (hENT1) and human concentrative nucleoside transporter (hCNT) 1 and 3 proteins to permeate through the plasma membrane.[5] After its entry into the cell, GEM is phosphorylated by deoxycytidine kinase to GEM triphosphate, a metabolite which is then incorporated into DNA mimicking deoxycytidine triphosphate. Following incorporation, GEM inhibits DNA polymerase, leading to terminated DNA synthesis and DNA repair.[6] Despite GEM's therapeutic promise, its clinical potential is hampered by its serious side effects such as myelosuppression, pulmonary toxicity, and gastrointestinal toxicity.[7] Furthermore, it has poor bioavailability and a short half-life (9−13 min for human plasma) because it is extensively deaminated to an inactive metabolite [2′,2′-difluorodeoxyuridine (dFdU)] by cytidine deaminase.[8] In order to improve oral bioavailability and efficacy, various GEM prodrugs have been developed, as summarized by Benoit et al.[9]

Integrins $\alpha_V\beta_3$, $\alpha_V\beta_5$, and $\alpha_5\beta_1$, are a family of cell surface receptors that are responsible for cell adhesion to the extracellular matrix and cell migration.[10,11] Integrins are overexpressed in cancer cells and have been recognized as targets for the development of anticancer drugs and drug delivery.[12] Among the various subtypes, integrin $\alpha_V\beta_3$ is particularly well studied. It recognizes the arginine−glycine−aspartic acid (RGD) moiety, and, for this reason, RGD peptides have been extensively employed for the development of targeted drug delivery systems.[13,14] To obtain a better clinical use of GEM, RGD-based delivery systems carrying GEM alone or in combination with other drugs have received the attention of researchers. For example, Yu et al. reported the development of RGD-conjugated albumin nanoparticles carrying GEM to pancreatic cancer cells.[15] Jin et al. demonstrated the co-delivery of GEM and paclitaxel in cRGD-modified nanoparticles with asymmetric lipid layers into breast cancer cells. The nanoparticles enhanced the drug accumulation in tumors compared to healthy tissues, and the antitumor effect of GEM was significantly improved.[16] In another study, Ji et al. reported an enzyme- and reduction-activatable RGD−GEM prodrug for targeted and image-guided cancer therapy.[17] Cochran et al. synthesized a GEM conjugate bearing an integrin-targeting knottin peptide that potently
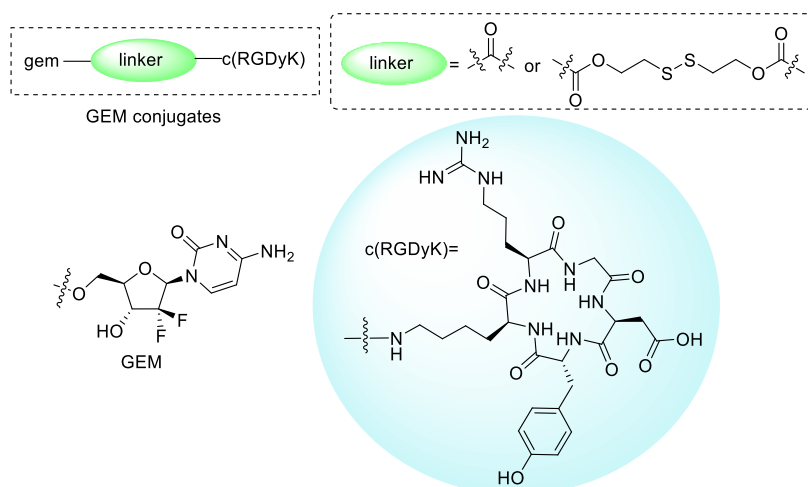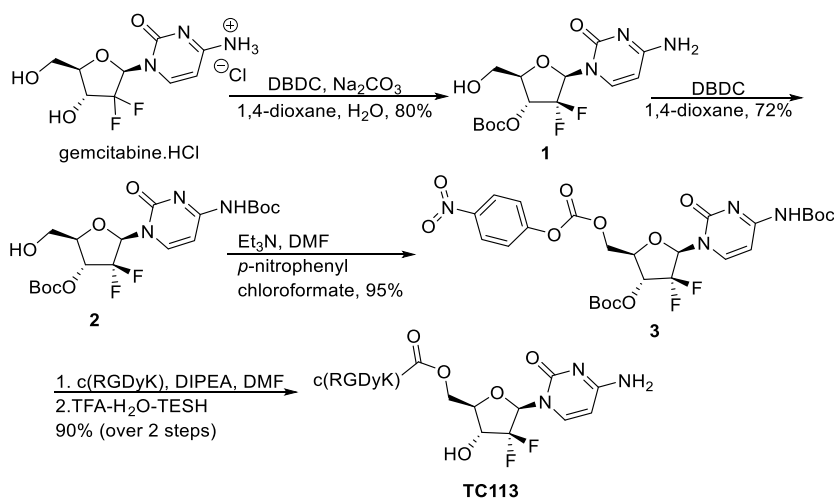
Figure 1. Molecular structures of c(RGDyK)-based conjugates of GEM studied in this work.

Scheme 1. Synthesis of Conjugate TC113

inhibited brain, breast, ovarian, and pancreatic cancer cell lines.[18]

Our group has conducted extensive studies synthesizing c(RGDyK) conjugates of known anticancer drugs for cancer imaging and treatment. We previously prepared c(RGDyK) conjugates of 5-FU, the alkylating agent POPAM, the natural products cucurbitacins,[19] and a Pt(II) complex for real-time drug delivery monitoring in cancer cells and photodynamic therapy (PDT).[20,21] It is known that the c(RGDyK) peptide has a high-affinity binding to $\alpha_v\beta_3$ integrins (IC$_{50}$ = 3.8 ± 0.42 nM) and has a lower binding to $\alpha_v\beta_5$ (IC$_{50}$ = 503 ± 55 nM), $\alpha_v\beta_6$ (IC$_{50}$ = 86 ± 7 nM), and $\alpha_5\beta_1$ integrins (IC$_{50}$ = 236 ± 45 nM).[22] Accumulative evidence demonstrates the association between integrin expression and the degree of dermal invasion in melanoma, risk of metastasis, and lung cancer.[23,24] In addition, melanoma tumors may metastasize to distant lymph nodes or other parts of the body such as the lung, liver, brain, and bone.[25] Thus, we designed new c(RGDyK) conjugates bearing GEM and explored their antiproliferative effects against the $\alpha_v\beta_3$ integrin expressing A549 lung cancer cells and metastatic WM266.4 human melanoma cells. GEM is attached to the c(RGDyK) peptide through a carbamate or a dithiol linker, as shown in Figure 1. Our results confirm that the synthesized c(RGDyK)−GEM conjugates effectively

inhibited the proliferation of lung cancer cells as well as the proliferation, invasiveness, and clonogenic ability of melanoma cells. Additionally, the cell uptake and *in vivo* pharmacokinetics of the lead c(RGDyK)−GEM conjugate was investigated.

■ RESULTS

Synthesis of c(RGDyK)−GEM Conjugates. The synthesis of c(RGDyK)−GEM conjugates is outlined in Scheme 1. The deprotected GEM **2** was prepared from GEM·HCl, following a two-step procedure, according to Guo and Gallo.[26] Compound **2** was activated with 4-nitrophenyl chloroformate and diisopropylethylamine (DIPEA) to produce carbonate **3**, which was then reacted with the c(RGDyK) peptide. The resultant c(RGDyK) conjugate was deprotected under acidic conditions to yield the product **TC113** in 90% yield over two steps. After the HPLC purification of the c(RGDyK)−GEM conjugate **TC113**, ESI-LCMS analysis revealed that the purity of the products was greater than 95%. The identity of compound **TC113** was confirmed by ¹H NMR, ¹³C NMR, and ESI-MS data.

The synthesis of conjugate **TC116** commenced with the protection of one hydroxyl group of commercially available 2,2′-dithiodiethanol with *tert*-butyldimethysilyl chloride (TBSCl) (Scheme 2). The resultant TBS ether **5** was then

Scheme 2. Synthesis of Conjugate TC116
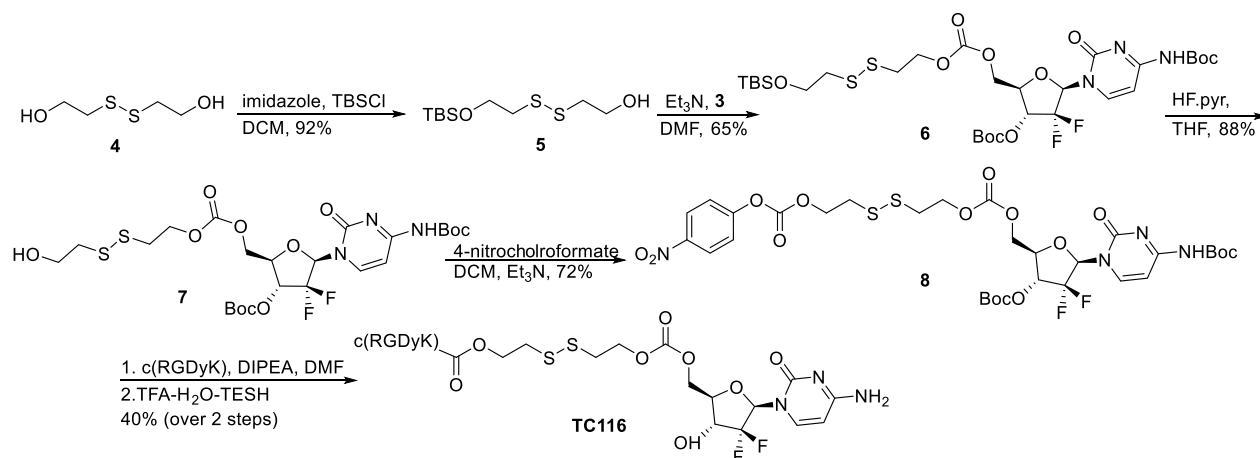
Scheme 3. Possible Release Mechanisms of GEM from Conjugate TC116 in the Presence of Esterases or under Reducing Conditions
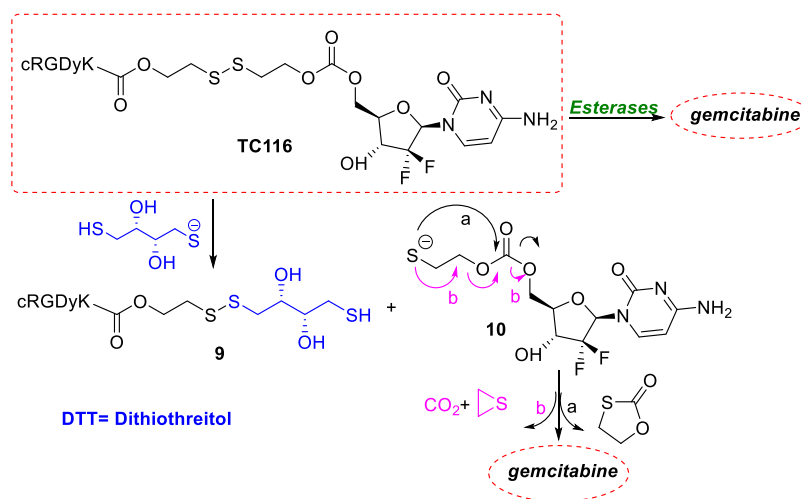

reacted with the activated carbonate **3**, forming the disulfide **6** in a moderate yield (65%). Desilylation of the TBS ether **7** with hydrogen fluoride/pyridine (HF/Py) in tetrahydrofuran (THF), followed by the reaction with 4-nitrophenyl chloroformate and Et₃N in dichloromethane (DCM) provided the desired p-nitrophenyl carbonate ester **8** in 72% yield. Compound **8** was coupled with the c(RGDyK) peptide, and the product was deprotected under acidic conditions to furnish conjugate **TC116** in 40% yield over two steps. The chemical structure of **TC116** was confirmed by ¹H NMR, ¹³C NMR, and ESI-MS data, with c(RGDyK) and GEM as controls.

Release of GEM from Conjugate TC116. In a biological system, the release of GEM from the conjugate **TC116** could be initiated by two possible pathways. The first pathway may involve the hydrolysis of **TC116** in the presence of esterases, as carbonates have often been reported as suitable substrates for esterases.[27,28] The second pathway could be initiated by the reducing conditions of biologically available thiols (e.g., glutathione) inside cells, where new disulfide bonds are created by thiol−disulfide exchange. Herein, the release mechanism of GEM in the presence of dithiothreitol (DTT) as a nucleophile from **TC116** has been examined (Scheme 3). To investigate the reductive cleavage of GEM, **TC116** was allowed to react with 1 equiv of DTT at room temperature,

and the reaction was monitored by using ¹H NMR and liquid chromatography−mass spectrometry (LC−MS) analyses (results shown in Figures 2 and 3). ¹H NMR data revealed the fast reduction of the disulfide bond with the subsequent release of GEM in the first 10 min. The reaction was completed after 2 h. In accordance with the ¹H NMR data, LC−MS showed that at the end of 2 h only a small quantity of **TC116** could be detected. In these experiments, GEM hydrochloride was used as a reference compound.

***In Vitro* Stability Studies of c(RGDyK)−GEM Conjugates.** Next, *in vitro* stability studies of c(RGDyK)−GEM conjugates were conducted using LC−MS techniques. The HPLC-UV and LC−MS/MS methods were initially developed for the identification and quantification of the c(RGDyK) peptide, **TC113**, **TC116**, and GEM. The stability of c(RGDyK)−GEM conjugates in two different pH values at 37 °C in a physiological pH of 7.4 and an acidic pH of 5.2 was then investigated at selected time points and analyzed using LC−MS.[29,30] The conjugate **TC113** remained stable after incubation at 37 °C under both pH values. **TC116** was found stable at pH = 5.2, while a slow hydrolysis was detected after 7 h in pH = 7.4. After 24 h of incubation, the residual concentration of **TC116** represented 85% of the initial **TC116** (Figure 4). This observation is related to the stability of the
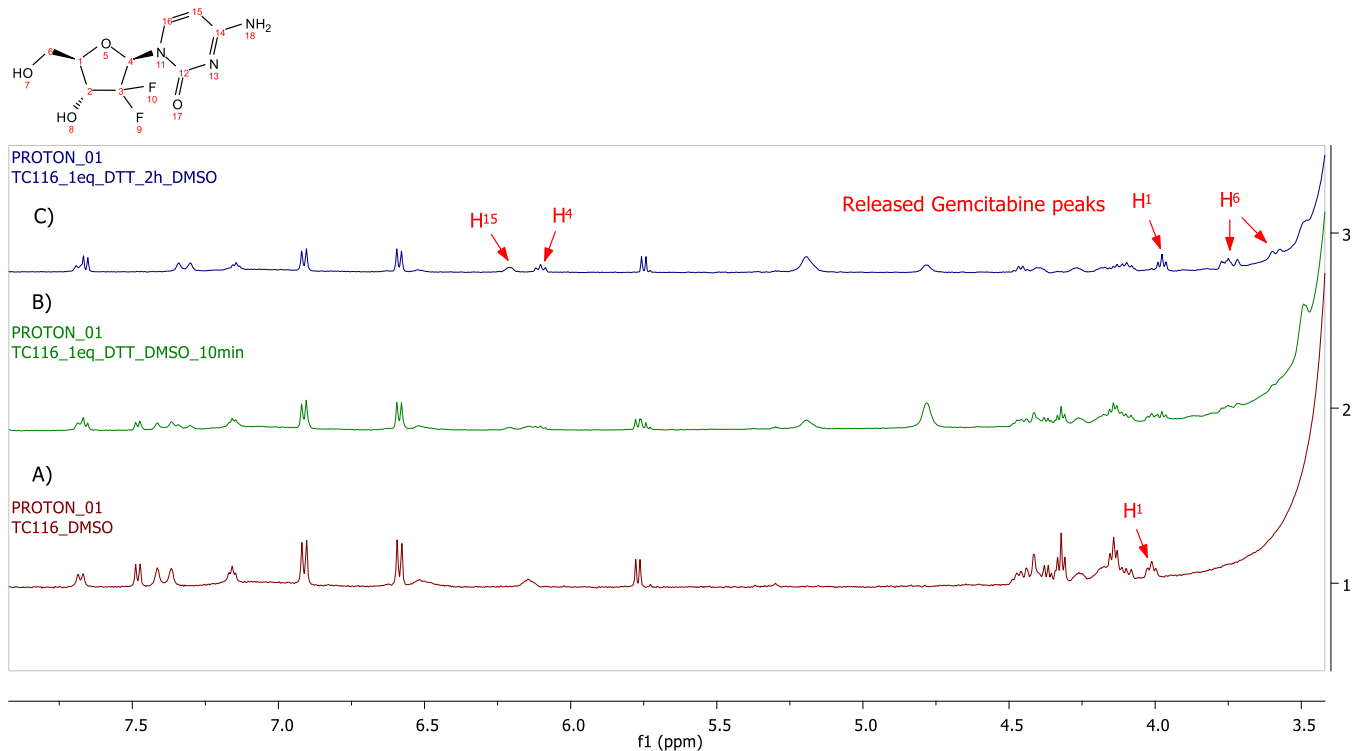
Figure 2. Release of GEM from conjugate **TC116**: ^{1}H NMR (500 MHz) spectra of conjugate **TC116** in (A) DMSO-d_6, (B) with 1 equiv DTT after 10 min, and (C) with 1 equiv DTT after 2 h.
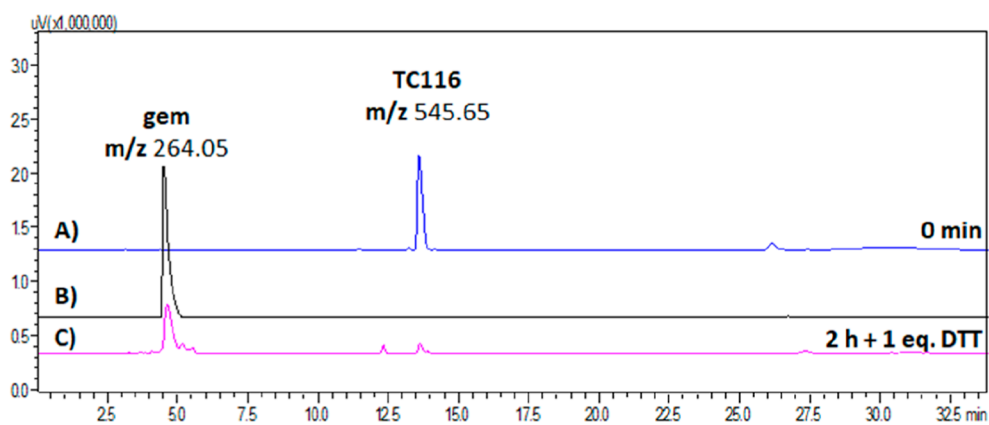
Figure 3. ESI-LC−MS chromatograms detected at 254 nm: (A) conjugate **TC116**, (B) GEM hydrochloride, and (C) release of GEM after 2 h of reaction of **TC116** with 1 equiv DTT in DMSO.
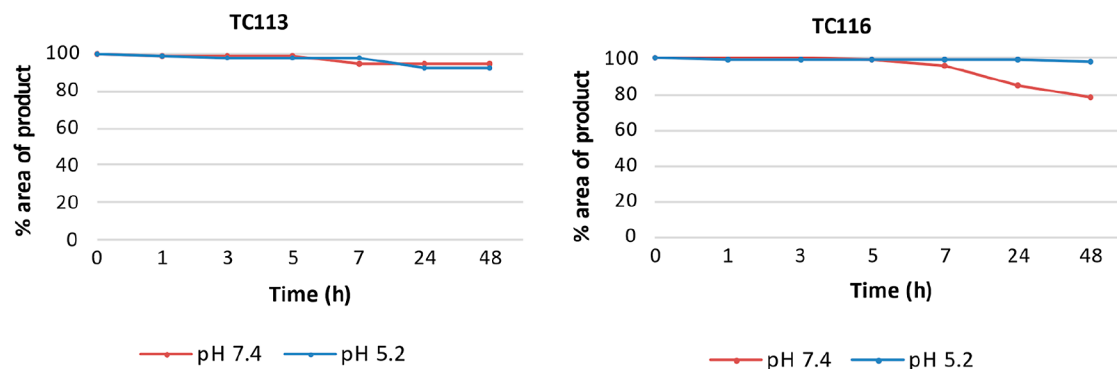
Figure 4. Chemostability of conjugates **TC113** and **TC116** by LC−MS analysis. Results are presented as mean ± SD of three independent experiments.
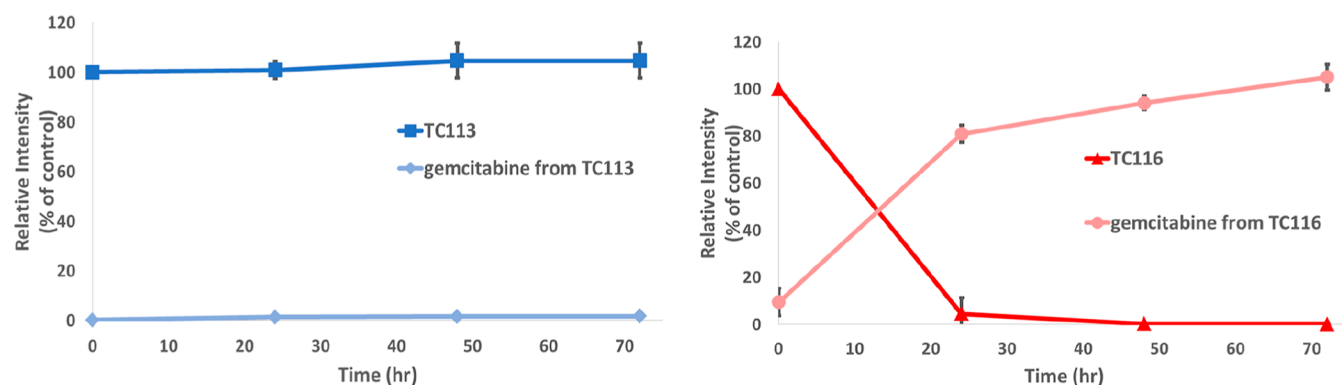
Figure 5. Stability of conjugates **TC113** and **TC116** in the cell culture medium DMEM (20 μg/mL).
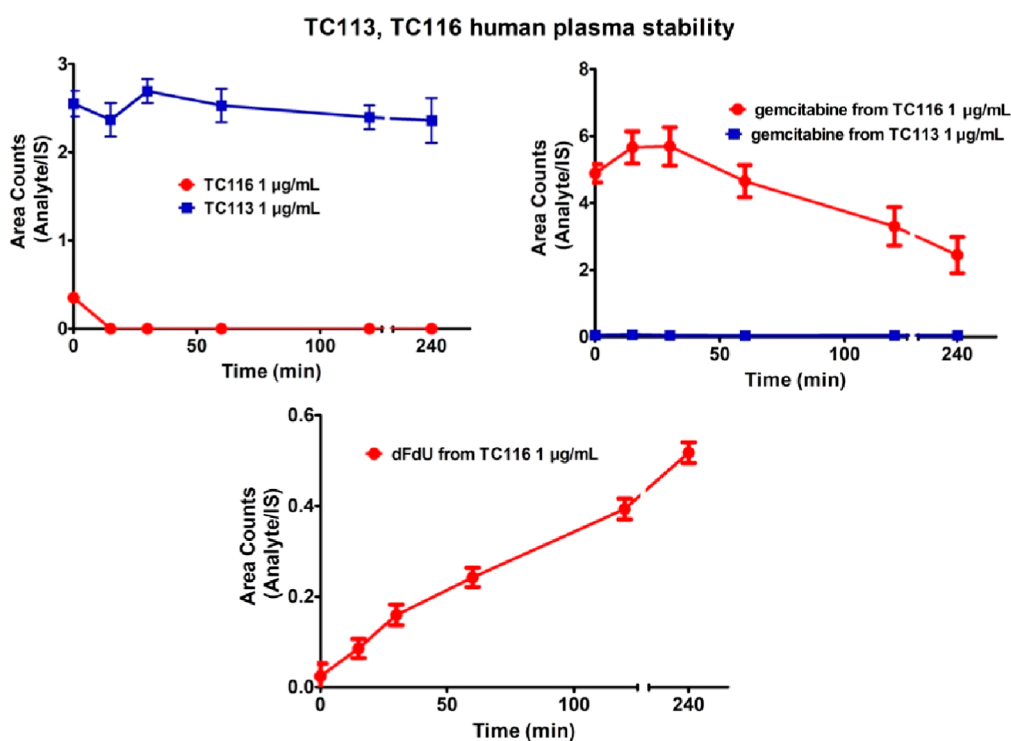

Figure 6. Stability profiles of conjugates **TC113** and **TC116** in human plasma (1 μg/mL).

carbonate bond at pH = 7.4 and is expected as the carbonate linkage is labile and susceptible to hydrolysis. In general, organic carbonates are less stable than carbamates and react easier with nucleophiles because nitrogen is a better electron donor than oxygen.

Stability studies in the medium DMEM-F12 and human plasma indicated that the **TC113** conjugate had a favorable profile over the **TC116** conjugate. The experiments in cell culture medium gave additional insights that are useful toward explaining the cytotoxicity induced by the conjugates. Stability tests in the medium DMEM-F12 showed that the **TC113** compound is stable over time in comparison to **TC116**, while **TC116** converts to GEM completely (Figure 5). In DMEM-F12, GEM release from **TC116** is accelerated and enhanced in comparison to that at pH 7.4 due to the presence of amino acids, such as cysteine, which participate in thiol−disulfide exchange reactions.

The stability profiles of **TC113** and **TC116** in human plasma is presented in Figure 6. Our findings reveal that **TC113** was stable over a period of 4 h in human plasma, while

TC116 was entirely unstable, releasing GEM even at $t = 0$ min. The deaminated metabolite of GEM, dFdU, was detected in the human plasma samples of **TC116,** and its concentration increased over time in proportion with the decrease of GEM. Human plasma contains various enzymes (esterases) and thiols such as glutathione that promote the cleavage of the carbonate bond, leading to the hydrolytic instability of **TC116**. Based on these findings, **TC113** was the most stable conjugate and was employed for further studies.

Cellular Uptake of c(RGDyK)−GEM Conjugate TC113 in A549 Cells. After the stability studies, the uptake efficiency of the c(RGDyK)−GEM conjugate **TC113** was investigated. A549 cells were incubated with 10 μM or 27.5 μM of **TC113**. Then, the cells were lysed, and the collected samples were analyzed at selected time points by LC−MS/MS analysis. As illustrated in Figure 7 the intracellular amount of **TC113** reached a peak at 5 ng/2 × 10^6 cells after 4 h of incubation. The concentration of dFdU also increased over time, and the highest intracellular concentration was achieved at approximately 4 ng/2 × 10^5 cells, following 24 h of **TC113**
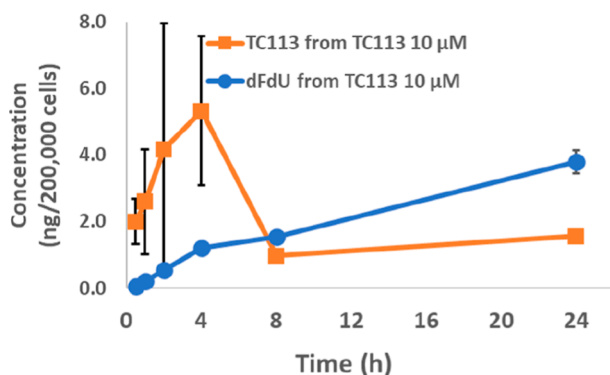
Figure 7. Cellular uptake of conjugate **TC113** in A549 cells.

incubation. GEM was also detected in this experiment in levels that were lower than the limit of quantification (0.05 ng/2 $\times$ 10^5 cells). Nevertheless, the dFdU (the inactive metabolite of GEM) levels measured could be considered as a surrogate marker of the presence of GEM in the cell as it is known that the majority of GEM is inactivated to dFdU after entering the cancer cell.

TC113 Cell Uptake through Integrin $\alpha_v\beta_3$. In a following step, the mechanism of **TC113** cell uptake was studied. A549 cells were incubated with **TC113** ($20\ \mu$M) in the presence or absence of either $10\ \mu$M c(RGDyK) or $10\ \mu$M cilengitide (both compounds are agonists of integrin $\alpha_v\beta_3$). The result presented in Figure 8 shows that in the presence of
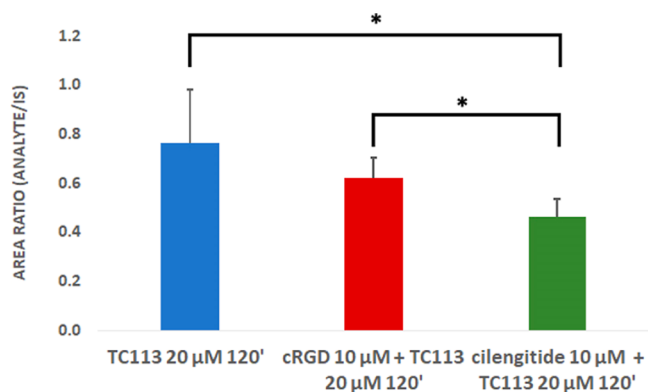

Figure 8. Cellular uptake of conjugate **TC113** in A549 cells in the presence or absence of other integrin $\alpha_v\beta_3$ agonists for: * $p < 0.05$.

the integrin $\alpha_v\beta_3$ competitor, **TC113** cell uptake is reduced, especially in the case of cilengitide co-incubation, suggesting that **TC113** cell uptake is mediated through integrin $\alpha_v\beta_3$.

■ BIOLOGICAL ACTIVITY STUDIES

Cytofluorimetric Assay of $\alpha_v\beta_3$ Expression on Lung Cancer and Melanoma Cells. To confirm that the selected cell lines, A549 and WM266.4, are suitable for investigating the integrin-mediated delivery of GEM, the levels of $\alpha_v\beta_3$ expression were evaluated. For comparison and better evaluation of the results, the $\alpha_V\beta_3$-negative myelogenous leukemia cell line K562 has also been employed as previously described.[31] Anti-integrin $\alpha_v\beta_3$−FITC-conjugated antibody was used, followed by the incubation of a goat antirabbit IgG FITC-conjugated secondary antibody. Cells exposed to a different primary antibody were analyzed separately using a BD flow cytometry system. In these assays, high levels of integrins $\alpha_v\beta_3$ were detected in both WM266.4 and A549 cells and very low levels in K562 cells (Figure 9).

Inhibition of Cell Adhesion to the $\alpha_v\beta_3$ Integrin Ligand Vitronectin by c(RGDyK)−GEM Conjugates. The c(RGDyK)−GEM conjugates, **TC113** and **TC116**, were evaluated for their ability to inhibit the adhesion to vitronectin (VN) of human melanoma cells WM266.4, lung cancer cells A549, and leukemia cells K562. This assay is used to examine whether the conjugates behave as integrin ligands and act as antagonists of integrin-mediated cell adhesion. More specifically, VN is an ECM protein that binds integrins $\alpha_v\beta_1$, $\alpha_v\beta_3$, $\alpha_v\beta_5$, or $\alpha II_b\beta_3$ regulating migration, tumor growth, and metastasis. A dose-dependent inhibition on WM266.4 cells was observed for the two compounds (Figure 10). In particular, in A549 cells, the **TC113** conjugate significantly inhibited cell adhesion compared to the equimolar concentration of **TC116** and c(RGDyK). Interestingly, in WM266.4 cells, the two conjugates inhibited cell adhesion, similar to what we observed after the exposure to the c(RGDyK) peptide. The IC$_{50}$ values of the c(RGDyK)−GEM conjugates **TC113** and **TC116** were calculated using the online tool Quest Graph IC$_{50}$ Calculator (AAT Bioquest, Inc., Sunnyvale, CA, USA). The IC$_{50}$ values were as follows: for A549 cells, IC$_{50}$ = 0.12 μM for **TC113**, IC$_{50}$ = 32 μM for **TC116**, and IC$_{50}$ > 100 μM for c(RGDyK). For WM266.4 cells, IC$_{50}$ = 0.21 μM for **TC113**, IC$_{50}$ = 9.5 μM for **TC116**, and IC$_{50}$ = 1.4 μM for c(RGDyK). Thus, the **TC113** conjugate is a potent inhibitor of cell adhesion mediated by $\alpha_v\beta_3$ integrin receptors. Low
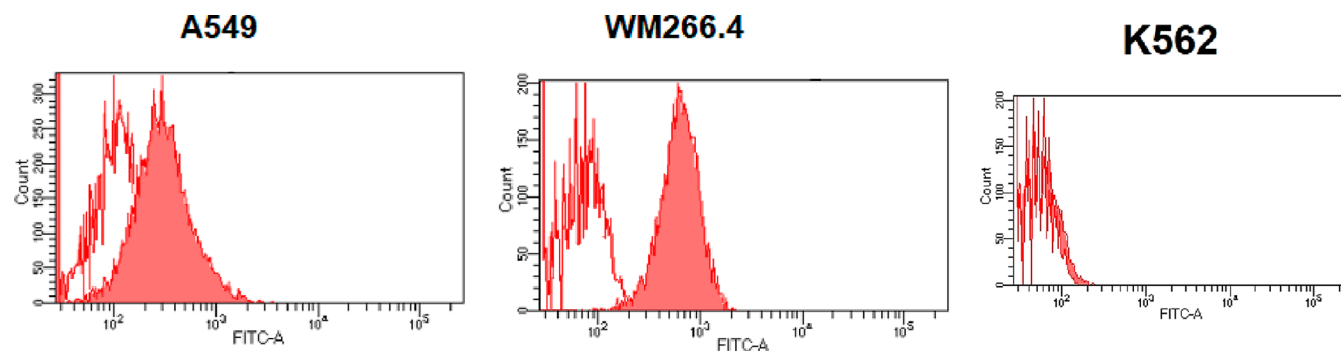
Figure 9. Cytofluorimetric analysis of $\alpha_v\beta_3$ protein expression on A549 cells and WM266.4. In each graph, the x axis represents the intensity of fluorescence (FITC-A) and the y axis represents the number of counted cells. Both cell lines were stained with the antirabbit $\alpha_v\beta_3$ antibody, followed by FITC-conjugated antirabbit immunoglobulin (full histograms). As a negative control (open histogram), cells were stained only with FITC-conjugated antirabbit immunoglobulin.
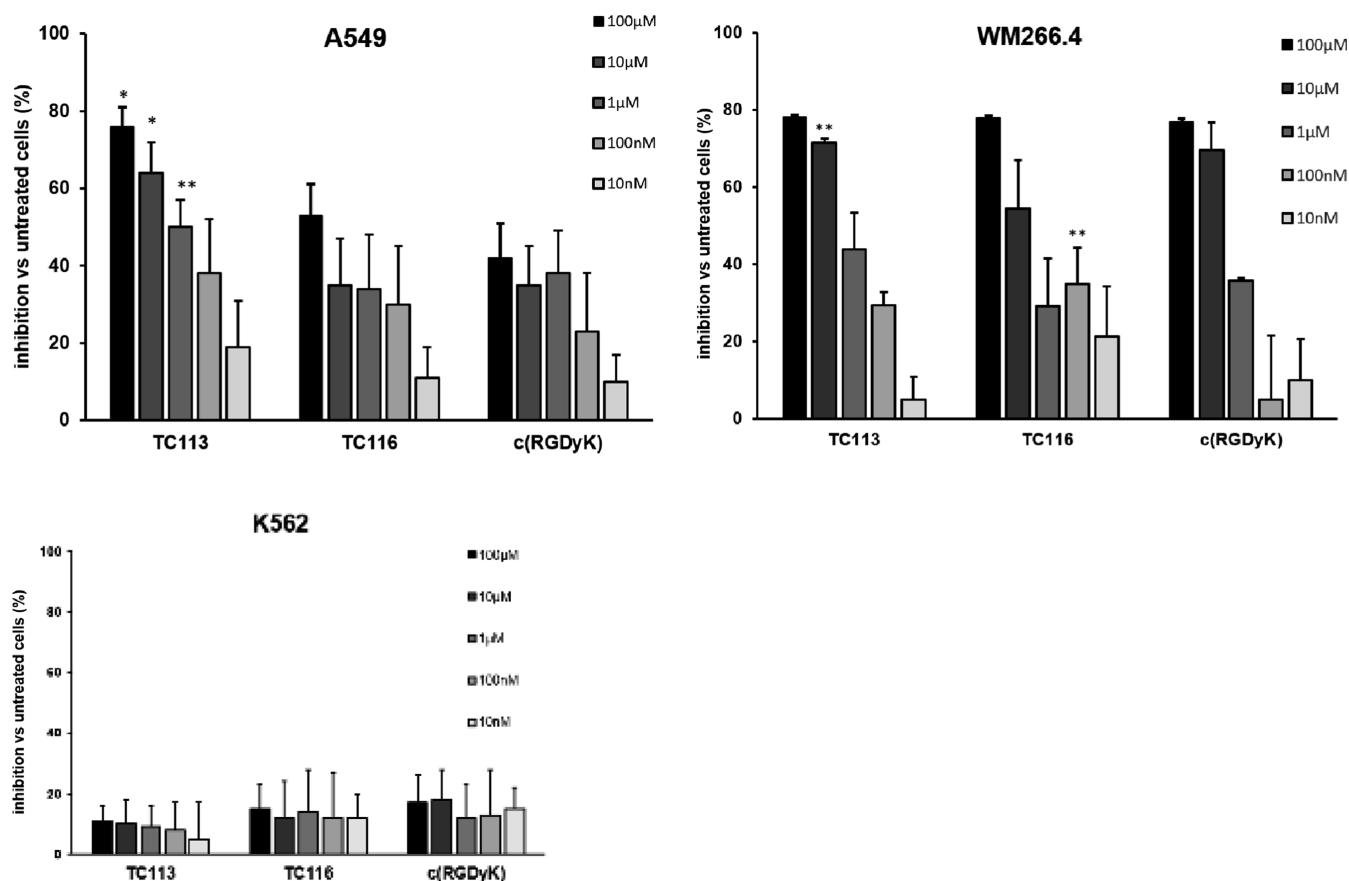
Figure 10. Inhibition of A549 and WM266.4 adhesion to VN substrate (5 μg/mL) in the presence of c(RGDyK)-based conjugates **TC113** and **TC116** or c(RGDyK). The inhibitory activity was calculated as the percentage of cell adhesion to VN in untreated cells and was expressed as mean $\pm$ SEM. Experiments were carried out in triplicate. *p <0.02 and **p <0.05 versus equimolar concentrations of other treatments by one-way ANOVA, followed by Tukey's multiple comparison test.

levels of adherent cells were measured for the $\alpha_V\beta_3$-negative myelogenous leukemia cells K562, as there is a small number of VN−integrin interactions.

Effects of c(RGDyK)-Based Conjugates TC113 and TC116 on Melanoma Cell Invasiveness, Cell Survival, and Clonogenic Ability. The effects of c(RGDyK)-based conjugates **TC113** and **TC116**, in comparison with the c(RGDyK) peptide, on human melanoma cell invasiveness were studied by the use of Matrigel-coated filters during a 4 h incubation. We found that the exposure of melanoma cells to a 10 μM dose of the different compounds reduced WM266.4 invasiveness and that the effects were comparable to what was observed by the use of the unconjugated c(RGDyK) peptide (Figure 11). The antiproliferative effect of c(RGDyK)-based conjugates **TC113** and **TC116** in comparison with GEM was evaluated by studying the induction of apoptosis/necrosis after 72 h of treatment at a 1 μM dose. We found that **TC113** and **TC116** induced necrosis in more than 20% of the population (21.7 and 31.1%, respectively), while GEM was able to induce necrosis in 12.4% of the population. Finally, we evaluated the clonogenic ability of cells that survived a 72 h treatment at 1 μM dose. We found that the number of colonies obtained from the cells exposed to **TC113** and **TC116** was strongly reduced compared to that of untreated cells and those exposed to GEM. Clonogenicity of WM266.4 cells treated with GEM was reduced to 46.6% compared to baseline, while after the treatment with **TC113** and **TC116,** clonogenicity of WM266.4 cells was reduced to 8.3 and 4.9%, respectively (Figure 11D).

Finally, we evaluated the percentages of growth inhibition in WM266.4 cells exposed for 24 h to different concentrations of **TC113**, **TC116,** and GEM, and we found IC$_{50}$ of 57.6 μM and >100 μM after the exposure to **TC113** and to **TC116**, respectively, while after the exposure to GEM, IC$_{50}$ was significantly lower (17.8 μM).

Effect of c(RGDyK)-Based Conjugates TC113 and TC116 on Lung Cancer Cell Proliferation. The antiproliferative effect of c(RGDyK)-based conjugates **TC113** and **TC116** in comparison with that of GEM was studied by the MTT assay in the non-small-cell lung cancer cell line A549 (Figure 12). The two conjugates demonstrated potent antiproliferative activities in the nanomolar range. In particular, **TC113** was less active than GEM (IC$_{50}$ = 18.8 nM) with an IC$_{50}$ of 678.5 nM, while **TC116** was comparable to GEM with an IC$_{50}$ of 30.6 nM (Table 1). Based on the stability studies, the observed cytotoxicity of **TC116** is partially attributed to the release of free GEM.

Pharmacokinetic Analysis of TC113. As **TC113** showed improved stability in comparison to **TC116**, combined with improved pharmacodynamic properties, it was selected as the lead compound for pharmacokinetic evaluation in mice. An aqueous formulation was thus developed, and **TC113** was administered in naïve mice at a dose that could be compared with previous pharmacokinetic studies performed by our group. Our results showed that **TC113** has promising pharmacokinetic properties as its administration resulted in a high blood concentration (8500 nM) achieved after 0.5 h
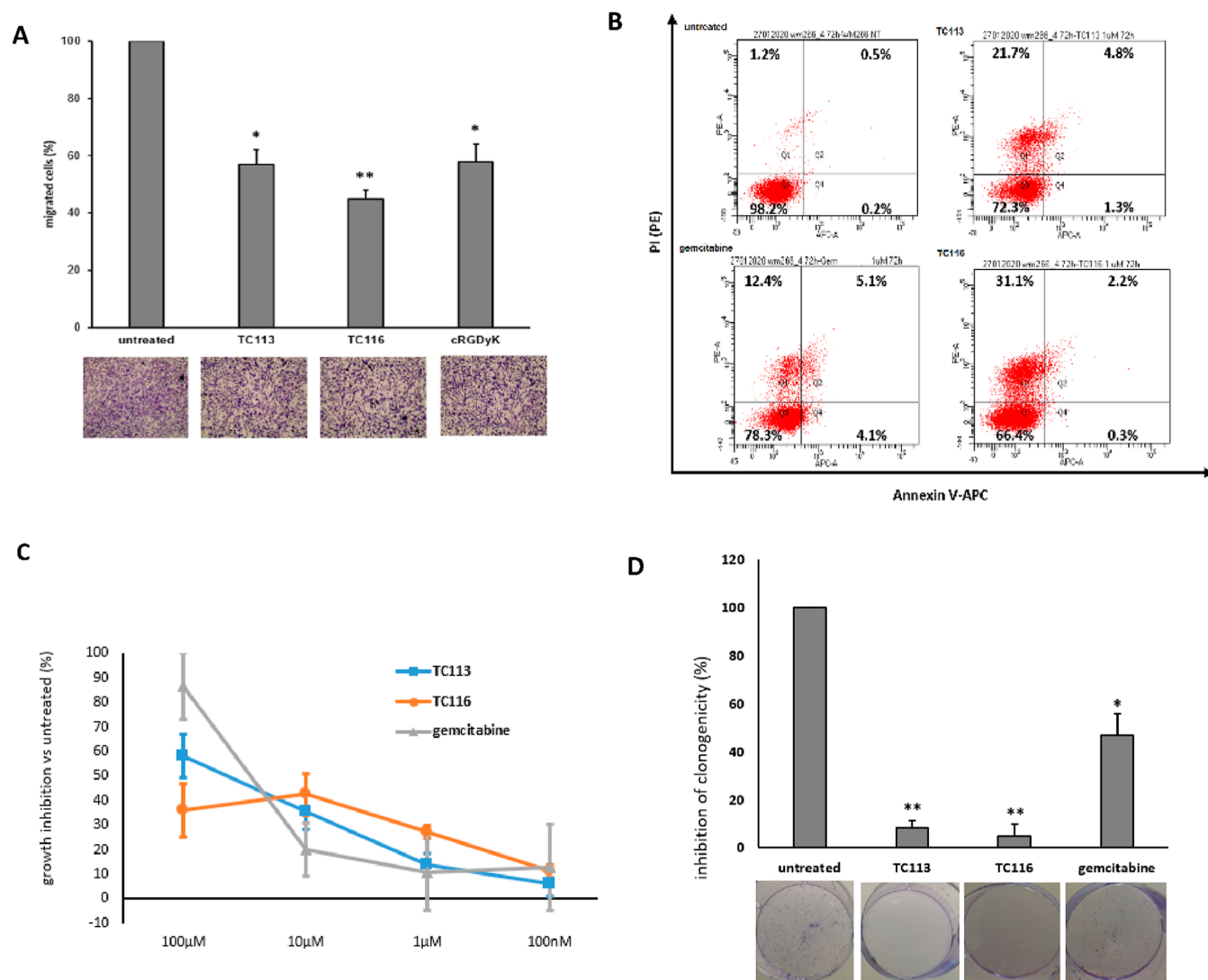
Figure 11. (A) Inhibition of WM266.4 invasiveness through Matrigel by c(RGDyK)-based conjugates **TC113** and **TC116** and c(RGDyK) (upper panel) and the corresponding representative images. (B) Annexin V and PI staining of WM266.4 cells after 72 h of exposure to c(RGDyK)-based conjugates **TC113** and **TC116** and GEM, 1 μM, and the corresponding percentages of cell population distribution are reported. (C) Growth inhibition of WM266.4 cells grown in the presence of different concentrations of **TC113**, **TC116,** and GEM for 24 h. Values are means of three independent experiments, with the standard errors of the mean represented by vertical bars. Asterisks indicate statistical significance versus untreated cells at * $p \leq 0.05$ and that versus c(RGDyK) and GEM at ** $p \leq 0.05$. (D) Clonogenic ability of WM266.4 cells after 72 h of exposure to c(RGDyK)-based conjugates **TC113** and **TC116** and GEM, 1 μM, percentage of clonogenic activity inhibition (upper panel), and representative images of cell colonies.

(Figure 13). According to the previous studies of its antiproliferative effect in cancer cells, the levels could potentially provide beneficial pharmacodynamics. In addition, **TC113** was found relatively stable for at least 1 h, while it released low levels of GEM. GEM's maximum blood concentration (750 nM) was achieved at 0.25 h. However, these levels were greatly decreased, suggesting that the administration of **TC113** does not result in high levels of circulating GEM, a drug characteristic that is often associated with off-target toxicities.

DISCUSSION AND CONCLUSIONS

We have synthesized two c(RGDyK)−GEM conjugates, and their stability was evaluated in cell culture medium and in human plasma. In general, **TC113** has a better stability profile related to **TC116**; therefore, it was further investigated *in vivo*. The conjugates bind to the integrin receptors and inhibit the cell adhesion to the $\alpha_V\beta_3$-integrin ligand VN similar to c(RGDyK). In addition, it was found that both conjugates (**TC113** and **TC116**) were able to significantly reduce WM266.4 melanoma cell invasiveness through Matrigel. Although Matrigel is not an RGD-containing substrate, integrin $\alpha_V\beta_3$ has a critical role in the grip-and-go migration and invasion modality of cancer cells due to its ability to bind Matrix Metalloprotease-2 and focalize its proteolitical activity. Thus, in order to highlight the role of the RGD moiety on cell migration and invasion, we evaluated the effect of the two different compounds on melanoma cells in comparison to the (unconjugated) c(RGDyK) peptide for 4 h at 10 μM concentration.[32] In addition, we evaluated the effect of **TC113** and **TC116** compounds on cell proliferation and survival, at a lower concentration (1 μM) and for a longer time, to highlight the effect of GEM. In these studies, we found that **TC113** and **TC116** were more efficient than GEM to inhibit
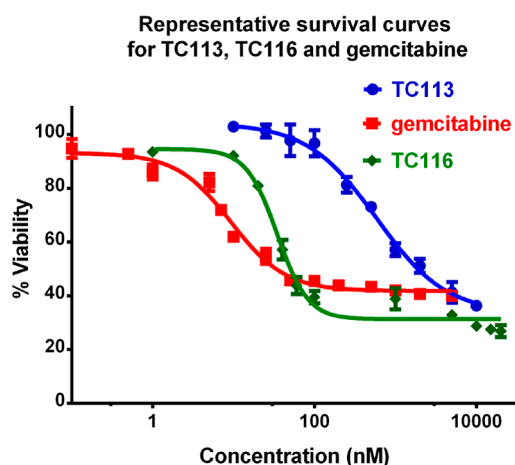
Figure 12. Cell viability curves assessed by the MTT assay in A549 cells.

Table 1. Antiproliferative Effect of TC113, TC116, and GEM in A549 Cells[a]

compound	GEM	TC113	TC116
IC$_{50}$ 72 h (nM)	18.8 ± 5.1	678.5 ± 261.4	30.6 ± 7.4

[a]IC$_{50}$ represents the half-maximal inhibitory concentration. Values shown represent means of at least three experiments (for GEM, $n = 4$; for **TC113**, $n = 3$; and for **TC116**, $n = 5$) performed in triplicate ± SD.

cell survival and clonogenic ability of melanoma cells. These results emphasize that the biological function of c(RGDyK)-conjugated compounds depends on the presence of the RGD moiety and on the selective delivery of GEM. The *in vitro* properties of c(RGDyK)−GEM conjugates were also evaluated against lung cancer cells A549 by the MTT assay method. Both conjugates exhibited potent cytotoxicity in the A549 cell proliferation assay, in which **TC116** exhibited a better inhibition activity, which is partially attributed to the release of GEM based on the stability study results.

The *in vivo* pharmacokinetic analysis of **TC113** demonstrated that **TC113** has a desirable pharmacokinetic profile in mice, as its administration leads to high **TC113** and low GEM circulation levels. The described multidimensional and integrated study on the discovery of a potent and targeted peptide conjugate of GEM can provide a platform for further research on the potential of molecules with anticancer activities in various types of cancers. Additional *in vivo* studies are warranted to establish the therapeutic efficacy of **TC113**.

◼ EXPERIMENTAL SECTION

General Experimental Details. All reactions were carried out under an atmosphere of Ar. All chemical reagents of high purity were purchased and used without further purification. The reactions were monitored by TLC, using UV light as a visualizing agent and aqueous ceric sulfate/phosphomolybdic acid, ethanolic *p*-anisaldehyde solution, potassium permanganate solution, and heat as developing agents. The ^{1}H and ^{13}C NMR spectra were recorded at 500 and 125 MHz (Agilent), with tetramethylsilane as an internal standard (IS). Chemical shifts are indicated in δ values (ppm) from internal reference peaks (TMS ^{1}H 0.00; CDCl$_3$ ^{1}H 7.26, ^{13}C 77.00; DMSO-d_6 ^{1}H 2.50, ^{13}C 39.51). Melting points (mp) are uncorrected. High-resolution mass spectra (HRMS) were recorded on a Waters Synapt G2 HDMS (Waters, UK) mass spectrometer with an electrospray source-acquired positive and negative ion data over a mass range of
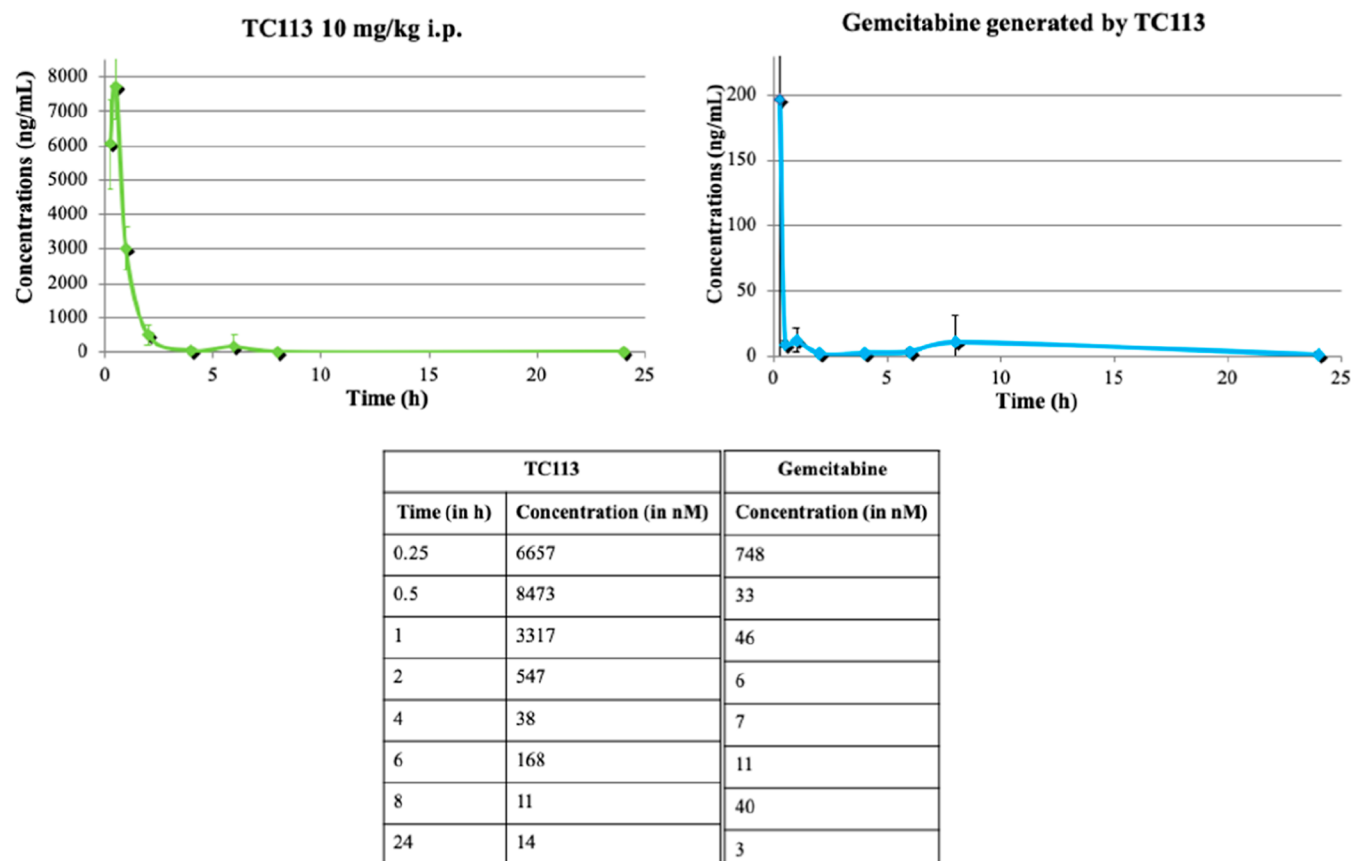
50−2000 *m/z* units. Microwave reactions were carried out in a Biotage Initiator microwave system 2.0 (400 W, operating at 2.45 GHz). HPLC purification using a C18 analytical (Gracesmart RP 18, 4.6 mm × 250 mm) column was performed with Scientific Systems Inc. instrumentation comprising 4-Q Grad pumps connected to a diode array (UV−vis Thermo Finnigan SpectraSYSTEM UV6000LP detector, Lab Alliance (New York, USA). The LC−MS spectra were recorded on a LC-20AD Shimadzu connected to Shimadzu LCMS-2010EV equipped with a C18 analytical column (Reprospher 100 C18-DE, 5 μm 250 × 4.6 mm, Dr Maisch GmbH). HR-MS was performed with a Thermo Scientific system where a Dionex Ultimate 3000 RSLC was coupled to a Q Exactive Focus mass spectrometer with an electrospray ion (ESI) source. An Acquitz UPLC BEH C8, 150 × 2.1 mm, 1.7 μm column equipped with a VanGuard Pre-Column BEH C8, 5 × 2.1 mm, 1.7 μm (Waters, Germany) was used for separation. At a flow rate of 250 μL/min, the gradient of (A) H$_2$O + 0.1% FA and (B) acetonitrile (ACN) + 0.1% FA was held at 10% B for 1 min and then increased to 95% B over 4 min. It was held there for 1.2 min before the gradient was decreased to 10% B over 0.3 min where it was held for 1 min. The purity of all final conjugates was determined to be ≥95% by analytical HPLC using the method presented in the Supporting Information. The mass spectrum was measured in both positive and negative modes in the range 120−1000 or 500−1500 *m/z*. UV spectrum was recorded at 254 nm.

(2R,3R,5R)-5-(4-Amino-2-oxopyrimidin-1(2H)-yl)-4,4-difluoro-2-(hydroxymethyl)tetrahydrofuran-3-yl *tert*-Butyl Carbonate (1). To a stirred mixture of GEM·HCl (60 mg, 0.2 mmol) and Na$_2$CO$_3$ (106 mg) in 4 mL dioxane and 1 mL water was added DBDC (44 mg, 0.2 mmol), and the resulting mixture was stirred at 24 °C for 48 h. The reaction was quenched with 2 mL of water, and the mixture was extracted with EtOAc. The organic extracts were washed with water (5 mL) and brine (5 mL), dried over Na$_2$SO$_4$, and concentrated to dryness under reduced pressure. The residue was purified by silica gel column chromatography (eluent: DCM/acetone/MeOH = 2/3/0.02) to give **1** (58 mg, 80% yield) as a white solid. The spectral data were in accordance with those reported in the literature.[26] **1**: ^{1}H NMR (500 MHz, (CD$_3$)$_2$CO): δ 7.72 (d, J = 7.6 Hz, 1H), 6.24 (t, J = 9.0 Hz, 1H), 5.98 (d, J = 7.6 Hz, 1H), 5.18 (dt, J = 13.1, 6.7 Hz, 1H), 4.37−4.02 (m, 3H), 3.90 (dd, J = 12.8, 2.3 Hz, 1H), 3.75 (dd, J = 12.8, 3.6 Hz, 1H), 1.42 (s, 9H); ^{13}C NMR (126 MHz, (CD$_3$)$_2$CO): δ 162.6, 152.2, 148.2, 138.1, 118.0, 91.9, 80.7, 80.6, 75.5, 68.8, 55.8, 23.3.

tert-Butyl(1-(4-((_tert_-butoxycarbonyl)oxy)-3,3-difluoro-5-(hydroxymethyl)tetrahydrofuran-2-yl)-2-oxo-1,2-dihydropyrimidin-4-yl)carbamate (2). To a stirred solution of **1** (35 mg, 0.095 mmol) in 3.8 mL dioxane was added DBDC (109 μL, 0.475 mmol). The reaction mixture was then stirred at 37 °C for 72 h. The solvent was removed under reduced pressure, the residue was washed with 0.95 mL hexane, and the residue was purified by flash chromatography (eluent: DCM/acetone = 50:1) to afford **2** (32 mg, 72% yield) as a white solid. The spectral data were in accordance with those reported in the literature.[26] **2**: ^{1}H NMR (500 MHz, (CD$_3$)$_2$CO): δ 9.26 (br, 1H), 8.16 (d, J = 7.6 Hz, 1H), 7.25 (d, J = 7.6 Hz, 1H), 6.36 (t, J = 8.5 Hz, 1H), 5.46−5.11 (m, 1H), 4.59 (br, 1H), 4.48−4.17 (m, 1H), 4.01 (d, J = 12.3 Hz, 1H), 3.87 (d, J = 12.3 Hz, 1H); ^{13}C NMR (126 MHz, (CD$_3$)$_2$CO): δ 164.7, 155.1, 152.8, 152.7, 145.6, 122.6, 95.8, 85.8, 84.4, 82.6, 80.6, 73.4, 60.6, 28.2, 27.7.

tert-Butyl(1-((2R,4R,5R)-4-((_tert_-butoxycarbonyl)oxy)-3,3-difluoro-5-((((4-nitrophenoxy)carbonyl)oxy)methyl)-tetrahydrofuran-2-yl)-2-oxo-1,2-dihydropyrimidin-4-yl)-carbamate (3). To a stirred solution of **2** (15 mg, 0.032 mmol) in dry DCM (0.6 mL) and triethylamine (18 μL, 0.13 mmol), at 0 °C under argon, was added 4-nitrophenyl chloroformate (10 mg, 0.049 mmol). As the solution turned yellow, the mixture was stirred at room temperature for 3 h. The solvent was removed under reduced pressure, and the residue was purified by flash chromatography (eluent: DCM/acetone = 50:1) to afford **3** (19 mg, 95% yield) as a white solid. **3**: ^{1}H NMR (500 MHz, (CD$_3$)$_2$CO): δ 9.27 (s, 1H), 8.39 (d, J = 9.0 Hz, 2H), 8.05 (d, J = 7.6 Hz, 1H), 7.63 (d, J = 9.0 Hz, 2H), 7.29 (d, J = 7.6 Hz, 2H), 6.41 (br, 1H), 5.51 (br, 1H), 4.83 (dd, J =

PK of TC113 10 mg/kg i.p. in male C57BL/6 mice

	TC113	Gemcitabine
Time (in h)	Concentration (in nM)	Concentration (in nM)
0.25	6657	748
0.5	8473	33
1	3317	46
2	547	6
4	38	7
6	168	11
8	11	40
24	14	3

Figure 13. Pharmacokinetic evaluation of **TC113** and GEM: GEM's maximum blood concentration was achieved at 0.25 h (750 nM). Similarly, **TC113** reached the highest blood concentration at 0.5 h (8500 nM).

12.2, 2.7 Hz, 1H), 4.78 (dd, J = 12.2, 5.4 Hz, 1H), 4.66 (br, J = 7.0 Hz, 1H), 1.53 (s, 9H), 1.52 (s, 9H); ^{13}C NMR (126 MHz, $(CD_3)_2CO$): δ 164.9, 156.6, 154.9, 153.2, 152.8, 152.6, 146.7, 146.1, 126.2, 123.3, 122.3, 96.1, 86.6, 84.8, 82.7, 77.8, 74.2, 67.9, 28.3, 27.8; ESI-HRMS m/z for $C_{26}H_{31}F_2N_4O_{12}$ $[M + H]^+$, calcd 629.1907; found, 629.1903.

Conjugate TC113. To a solution of c(RGDyK) (5 mg, 8 μmol) in dry dimethylformamide (DMF) (2 mL), DIPEA was added (5 μL, 0.048 mmol), following the addition of the activated ester **3** (6 mg, 9.7 μmol). The reaction was left stirring at room temperature for 48 h and monitored by LC−MS. The solvent was evaporated *in vacuo* to give the crude Boc-protected product, which was then treated with 0.3 mL of a solution of TFA−H_2O−TES (95:2.5:2.5). The resulting solution was stirred at room temperature for 2 h and subsequently concentrated through freeze-drying to give the crude product which was purified by reverse-phase HPLC. **TC113** was isolated in 90% yield (6.5 mg, white solid). The purity of the conjugate was confirmed by LC−MS and mass spectrometry (linear gradient from 90% H_2O to 10% ACN; 0.1% HCOOH; over 35 min; flow rate: 0.4 mL/min; R_t = 13.5 min). **TC113**: ^{1}H NMR (500 MHz, CD_3COCD_3/D_2O, 1:1): δ 8.26 (s, 2H), 7.49 (d, J = 7.6 Hz, 1H), 6.96 (d, J = 8.2 Hz, 2H), 6.67 (d, J = 8.1 Hz, 2H), 6.14 (t, J = 8.1 Hz, 1H), 5.96 (d, J = 7.5 Hz, 1H), 4.63 (t, J = 6.8 Hz, 1H), 4.46 (m, 1H), 4.32 (dd, J = 39.8, 31.4 Hz, 1H), 4.23 (dd, J = 12.5, 5.1 Hz, 1H), 4.16 (d, J = 15.1 Hz, 1H), 4.06 (s, 1H), 3.83 (d, J = 4.0 Hz, 1H), 3.36 (d, J = 14.9 Hz, 1H), 3.12 (m, 2H), 2.95 (m, 2H), 2.86−2.75 (m, 2H), 2.69−2.60 (m, 1H), 2.52 (dd, J = 16.3, 6.2 Hz, 1H), 1.80 (m, 1H), 1.58 (m, 2H), 1.46 (m, 3H), 1.24 (m, 2H), 1.01−0.78 (m, 2H); ^{13}C NMR (126 MHz, CD_3COCD_3/D_2O, 1:1): δ 174.5, 174.3, 173.2, 172.7, 171.8, 171.3, 166.8, 166.30, 157.6, 157.2, 156.4, 155.8, 141.8, 130.8, 127.8, 122.7, 115.7, 96.4, 84.9, 78.8, 70.6, 62.7, 55.7, 55.7, 52.7, 50.2, 43.9, 41.1,

40.5, 36.7, 35.8, 30.7, 29.0, 28.0, 25.1, 23.1; ESI-HRMS m/z for $C_{37}H_{51}F_2N_{12}O_{13}$ $[M − H]^-$, calcd 907.3510; found, 907.3515.

2-((2-((*tert*-Butyldimethylsilyl)oxy)ethyl)disulfanyl)ethan-1-ol (5). 2,2′-Dithiodiethanol (100 mg, 0.648 mmol) was dissolved in dry DCM (4 mL), and a solution of imidazole (44 mg, 0.648 mmol) in anhydrous DMF (0.1 mL) was added. Next, a solution of *tert*-butyldimethylsilyl chloride (98 mg, 0.648 mmol) in dry DCM (0.5 mL) was added, and the reaction mixture was stirred at room temperature for 18 h. Subsequently, imidazole (66 mg, 0.972 mmol) and *tert*-butyldimethylsilyl chloride (147 mg, 0.972 mmol) were added, and the mixture was stirred for another 18 h. The solvent was removed under reduced pressure, and the mixture was extracted with EtOAc. The organic extracts were dried over Na_2SO_4 and concentrated to dryness under reduced pressure. The residue was purified by silica gel column chromatography (eluent: hexane/EtOAc = 8:1) to give **5** (58 mg, 92% yield) as a colorless liquid. The spectral data were in accordance with those reported in the literature.[33] **5**: ^{1}H NMR (500 MHz, CDCl$_3$): δ 3.88 (t, J = 5.8 Hz, 2H), 3.86 (7, J = 5.8 Hz, 2H), 2.85 (t, J = 5.0 Hz, 2H), 2.83 (t, J = 5.8 Hz, 2H), 0.89 (s, 9H), 0.07 (s, 6H); ^{13}C NMR (126 MHz, CDCl$_3$): δ 61.8, 60.2, 41.3, 41.2, 25.8, 18.3, −5.3.

***tert*-Butyl(1-((2R,4R,5R)-4-((*tert*-butoxycarbonyl)oxy)-3,3-difluoro-5-(12,12,13,13-tetramethyl-3-oxo-2,4,11-trioxa-7,8-dithia-12-silatetradecyl)tetrahydrofuran-2-yl)-2-oxo-1,2-dihydropyrimidin-4-yl)carbamate (6).** To a stirring solution of **6** (15.3 mg, 0.057 mmol) in dry DMF (0.5 mL) under argon, Et$_3$N (17 μL, 0.011 mmol) is added, followed by the addition of **3** (35 mg, 0.057 mmol). The reaction mixture was left stirring for 48 h at 40 °C. The solvent was then removed under reduced pressure, and the residue was purified by silica gel chromatography (eluent: DCM/acetone = 10:1) to afford **6** (36.7 mg, 85%) as white foam. **6**: ^{1}H NMR (500

MHz, CDCl$_3$): δ 7.70 (d, J = 7.6 Hz, 1H), 7.29 (d, J = 7.7 Hz, 1H), 6.50−6.36 (m, 1H), 5.10 (d, J = 10.4 Hz, 1H), 4.50 (m, 2H), 4.43 (t, J = 6.8 Hz, 2H), 4.37 (m, 1H), 3.85 (t, J = 6.5 Hz, 2H), 2.95 (t, J = 6.8 Hz, 2H), 2.83 (t, J = 6.5 Hz, 2H), 1.50 (s, 18H), 0.88 (s, 9H), 0.06 (s, 6H); ^{13}C NMR (126 MHz, CDCl$_3$): δ 163.1, 154.5, 154.4, 151.4, 150.9, 144.1, 120.3, 95.6, 84.8, 84.0, 83.1, 77.2, 72.7, 66.4, 65.1, 61.6, 41.5, 36.6, 27.9, 27.5, 25.8, 18.3, −5.4; ESI-MS m/z for C$_{30}$H$_{50}$F$_2$N$_3$O$_{11}$S$_2$Si [M + H]$^+$, calcd 758.26; found, 758.00.

tert-Butyl(1-((2R,4R,5R)-4-((*tert*-butoxycarbonyl)oxy)-3,3-di-fluoro-5-((((2-((2-hydroxyethyl)disulfanyl)ethoxy)carbonyl)-oxy)methyl)tetrahydrofuran-2-yl)-2-oxo-1,2-dihydropyrimi-din-4-yl)carbamate (7). Compound 6 (28.5 mg, 0.038 mmol) was dissolved in THF (0.64 mL) and pyridine (175 μL). Subsequently, a solution of 1:2.3 HF/Py (75 μL:175 μL) was added. The reaction was left stirring overnight at room temperature and quenched with saturated NaHCO$_3$. The product was extracted with ethyl acetate. The organic layers were dried over Na$_2$SO$_4$, filtered, and concentrated under vacuum. The residue was purified by silica gel chromatography (eluent: DCM/acetone = 4:1) to afford 7 (24 mg, 98%) as white foam. 7: ^{1}H NMR (500 MHz, CDCl$_3$): δ 7.71 (d, J = 7.5 Hz, 1H), 7.29 (d, J = 7.6 Hz, 1H), 6.55−6.37 (m, 1H), 5.12 (d, J = 10.7 Hz, 1H), 4.59−4.40 (m, 4H), 4.35 (s, 1H), 3.88 (t, J = 5.7 Hz, 2H), 2.97 (t, J = 6.5 Hz, 2H), 2.89 (t, J = 5.7 Hz, 2H), 1.50 (s, 18H); ^{13}C NMR (126 MHz, CDCl$_3$): δ 163.2, 154.6, 154.5, 151.4, 151.1, 144.2, 120.4, 95.7, 84.9, 84.2, 83.2, 77.2, 72.5, 66.3, 65.1, 60.2, 41.6, 36.6, 27.9, 27.5; ESI-MS m/z for C$_{24}$H$_{36}$F$_2$N$_3$O$_{11}$S$_2$ [M + H]$^+$, calcd 644.1759; found, 644.1753.

tert-Butyl(1-((2R,4R,5R)-4-((*tert*-butoxycarbonyl)oxy)-3,3-di-fluoro-5-(12-(4-nitrophenoxy)-3,12-dioxo-2,4,11-trioxa-7,8-dithiadodecyl)tetrahydrofuran-2-yl)-2-oxo-1,2-dihydropyri-midin-4-yl)carbamate (8). To a solution of 7 (24.6 mg, 0.038 mmol) in dry DCM (0.8 mL) and Et$_3$N (32 μL, 0.028 mmol) at 0 °C, 4-nitrophenyl chloroformate (30.6 mg, 0.0152 mmol) is added. The reaction is left stirring at room temperature for 2 h. The product is purified by silica gel chromatography (eluent: DCM/acetone = 15:0.5) to afford 27.2 mg (88%) of 8 as white foam. 8: ^{1}H NMR (500 MHz, CDCl$_3$): δ 8.28 (d, J = 8.9 Hz, 2H), 7.70 (d, J = 7.5 Hz, 1H), 7.39 (d, J = 8.9 Hz, 2H), 7.28 (d, J = 7.5 Hz, 1H), 6.48−6.41 (m, 1H), 5.11 (d, J = 10.8 Hz, 1H), 4.55 (t, J = 6.5 Hz, 2H), 4.50 (m, 2H), 4.46 (t, J = 6.5 Hz, 2H), 4.37 (m, 1H), 3.06 (t, J = 6.5 Hz, 2H), 3.02 (t, J = 6.5 Hz, 2H), 1.51 (s, 18H); ^{13}C NMR (126 MHz, CDCl$_3$): δ 163.0, 155.4, 154.5, 154.4, 152.3, 151.4, 150.9, 145.5, 144.2, 125.3, 121.8, 120.3, 95.6, 84.9, 83.9, 83.2, 77.4, 72.7, 66.8, 66.2, 65.2, 36.8, 36.7, 27.9, 27.5; ESI-MS m/z for C$_{31}$H$_{39}$F$_2$N$_4$O$_{15}$S$_2$ [M + H]$^+$, calcd 809.1821; found, 809.1819.

Conjugate TC116. To a solution of c(RGDyK) (5 mg, 8 μmol) in dry DMF (1.5 mL), DIPEA was added (5 μL, 0.049 mmol), following the addition of the activated ester 8 (7.76 mg, 8 μmol). The reaction was left stirring at room temperature for 48 h and monitored by LC−MS. The solvent was evaporated *in vacuo* to give the crude Boc-protected product, which was then treated with 0.3 mL of a solution of TFA−H$_2$O−TES (95:2.5:2.5). The resulting solution was stirred at room temperature for 1.5 h and subsequently concentrated through freeze-drying to give the crude product which was purified by reverse-phase HPLC. TC116 was isolated in 65% yield (5.59 mg, white solid). The purity of the conjugate was confirmed by LC−MS and mass spectrometry (linear gradient from 90% H$_2$O to 10% ACN, 0.1% HCOOH, over 35 min, flow rate: 0.4 mL/min, R$_t$ = 14 min). TC116: ^{1}H NMR (500 MHz, CD$_3$OD/D$_2$O, 1:1): δ 8.27 (s, 2H), 7.61 (d, J = 7.7 Hz, 1H), 7.06 (d, J = 8.3 Hz, 2H), 6.78 (d, J = 8.1 Hz, 2H), 6.22 (t, J = 7.7 Hz, 1H), 6.05 (d, J = 7.6 Hz, 1H), 4.74 (t, J = 7.1 Hz, 1H), 4.62 (d, J = 12.2 Hz, 1H), 4.57−4.43 (m, 4H), 4.31 (m, 6H), 3.83 (m, 1H), 3.44 (d, J = 14.8 Hz, 1H), 3.25−3.12 (m, 2H), 3.08−2.90 (m, 7H), 2.85 (dd, J = 16.6, 8.3 Hz, 2H), 2.66 (dd, J = 16.6, 6.4 Hz, 1H), 1.90−1.80 (m, 1H), 1.65 (m, 2H), 1.58−1.41 (m, 3H), 1.40−1.25 (m, 2H), 0.95 (m, 2H); ^{13}C NMR (126 MHz, CD$_3$OD/D$_2$O 1:1): δ 175.3, 175.2, 174.1, 173.5, 172.5, 172.2, 166.5, 166.4, 158.9, 157.9, 156.8, 156.1, 142.3, 131.4, 128.5, 123.0, 116.4, 97.1, 85.8, 79.2, 70.9, 67.3, 66.5, 63.6, 56.6, 56.4, 53.4, 50.9, 44.6, 41.6, 40.9, 38.4, 37.7, 37.4, 36.1, 31.3, 29.5, 28.8, 25.7, 23.8 (two carbons are missing due to

overlapping); ESI-MS m/z for C$_{42}$H$_{57}$F$_2$N$_{12}$O$_{16}$S$_2$ [M − H]$^−$, calcd 1087.3425; found, 1087.3425.

Development of an HPLC−UV Method to Simultaneously Detect and Quantify GEM and TC113/TC116. An HPLC method has been established for the identification and simultaneous quantification of each GEM conjugate with GEM. A C-18 column (4.6 × 150 mm, 5 μm) was used at a flow rate of 1 mL/min for sample retention. The mobile phases consist of solutions A (100% H$_2$O, 2 mM ammonium acetate, and 0.1% formic acid) and B (90% ACN, 10% H$_2$O, 2 mM ammonium acetate, and 0.1% formic acid).

Development of a LC−MS/MS Method to Simultaneously Detect and Quantify GEM and TC113. GEM and TC113 were characterized and quantified by LC−MS/MS. An Agilent Zorbax Eclipse XDB-C-18 column (4.6 × 150 mm, 5 μm) at a flow rate of 1 mL/min was used for separation. Mass spectrometry was performed on an API 4000 QTRAP LC−MS/MS system fitted with a TurboIonSpray source and a hybrid triple quadrupole/linear ion trap mass spectrometer. A set of working calibration standards containing 1−2000 ng/mL for GEM and 25−10 000 ng/mL for TC113 was prepared. Capecitabine was used as IS.

Chemostability Experiments. Chemostability tests were performed at two different pH values, 7.4 and 5.2, in order to examine the stability of the conjugates. Stock solutions of the conjugates were prepared (0.33−0.66 mM) by dissolving 0.25−0.3 mg of each conjugate with 5 μL of DMSO and 500 μL of the relevant buffer solution (phosphate buffer pH 7.4 or acetate buffer pH 5.2). The solution was incubated at 37 °C. Samples were collected and analyzed by LC−MS at 0, 1, 3, 5, 7, 24, and 48 h. Results are presented as mean ± SD for three independent experiments.

***In Vitro* Stability in Cell Culture Medium (DMEM-F12).** 20 μg/mL of TC113, TC116, or GEM was incubated in a cell culture medium (DMEM-F12) at 37 °C. The samples (triplicates of 40 μL) were collected at selected time points (0, 0.5, 1, 2, 4, 6, 8, and 24 h) and were stored at −80 °C after mixing with 160 μL of the initial mobile phase (90% H$_2$O, 10% ACN, 2 mM ammonium acetate, and 0.1% formic acid). The samples were analyzed using LC−MS/MS.

***In Vitro* Stability of Human Plasma.** 20 μg/mL of either TC113, TC116, or GEM was incubated in human plasma. Samples (triplicates of 50 μL) were collected at selected time points (0, 0.5, 1, 2, 4, 6, 8, and 24 h) and were stored at 80 °C after mixing with 150 μL of ACN. The samples were then extracted using protein precipitation and analyzed using LC−MS/MS.

Determination of Intracellular Concentrations of TC113. Cells (A549) were plated in 24-well plates at a density of 2 × 10^5 cells per well. The cells were then incubated with TC113 (10 μM) for selected time points (1, 2, 4, 8, and 24 h). Incubations were terminated by removing the medium and washing the cells twice with ice-cold phosphate-buffered saline (PBS) to remove unbound TC113. The cells were then lysed by adding an ice-cold solution of ACN−water (3:2) and scraping the cell monolayer. The samples were subsequently vortexed, sonicated, and centrifuged for 3 min at 16 060g (Heraeus Biofuge Pico microcentrifuge, Thermo Scientific, Bonn, Germany). The supernatants were collected, evaporated, and stored at −20 °C until the day of analysis. Intracellular accumulation of TC113, GEM, and dFdU was determined by LC−MS/MS analysis using a stable IS as well as TC113, GEM, and dFdU standards for the construction of analytical standard curves. For the co-incubation studies of TC113 and cRGD or cilengitide, cells (A549) were plated in six-well plates at a density of 1 × 10^6 cells per well. The cells were then incubated with TC113 (20 μM) in the presence or absence of 10 μM c(RGDyK) or 10 μM cilengitide for 2 h. Incubations were terminated by removing the medium and washing the cells twice with ice-cold PBS to remove unbound TC113. The cells were then lysed by adding an ice-cold solution of ACN−water (3:2) and scraping the cell monolayer. The samples were subsequently vortexed, sonicated, and centrifuged for 3 min at 16 060g (Heraeus Biofuge Pico microcentrifuge, Thermo Scientific, Bonn, Germany). The supernatants were collected, evaporated, and stored at −20 °C until the day of analysis. Intracellular accumulation of TC113 was determined by LC−MS/MS analysis using a stable IS.

***In Vivo* Pharmacokinetic Evaluation.** For the pharmacokinetic experiments, a mouse serial tail bleeding protocol was developed using six C57BL/6 naive mice (average age = 8−10 weeks; average weight = 25 g/animal). All animals were weighed and fasted overnight before dosing. The animals were administered intraperitoneally 10 mg/kg **TC113** diluted in saline with a total volume of 200 μL/animal. A serial tail bleeding protocol was used for the collection of blood samples. Blood samples (10 μL) were collected at seven time points (0.15, 0.5, 1, 2, 4, 6, 8, and 24 h) in tubes containing 40 μL of sodium citrate (0.1 M, pH 4.5) and stored at −80 °C until the day of the analysis. Samples were prepared for quantification by protein precipitation and evaporation. **TC113** and GEM were quantified by LC−MS/MS analysis.

Cell Growth Assay. Cells (A549) were plated at a density of 5 × 10^3 cells per well on 96-well plates. After 24 h of incubation (37 °C, 5% CO_2), the cell medium was removed, and compounds were added at selected concentrations (e.g., 10−20 000 nM), followed by incubation for 72 h. The medium was then removed, and the MTT solution (0.3 mg/mL in PBS) was added to cells for 3 h, after which the MTT solution was removed, and the formazan crystals were dissolved in 100 μL of DMSO. The optical density was measured at 570 nm and a reference wavelength of 650 nm using an absorbance microplate reader (SpectraMax 190, Molecular Devices, Sunnyvale, CA, USA). The 50% cytostatic concentration (IC_{50}) was calculated using GraphPad Prism 7.0 (GraphPad Software, San Diego, CA, USA). Each value is the result of at least three experiments performed in triplicates.

Cytofluorimetric Assay of $\alpha_v\beta_3$ and $\alpha_v\beta_5$ Expression on Melanoma/A549 Cells. WM266.4 human melanoma cells were detached by a gentle treatment with Accutase, washed, and incubated for 1 h at 4 °C in the presence of a polyclonal antibody against the $\alpha_v\beta_3$ integrin receptor (1 μg each/50 μL PBS). We used a rabbit anti-(h,m,r) integrin $\alpha_v\beta_3$ (bs1310R Bioss USA), followed by incubation with 1 μL/50 μL PBS of goat antirabbit IgG FITC-conjugated (24549933 ImmunoTools Friesoythe, Germany) secondary antibody. Cells were analyzed using a BD flow cytometry system (FACS Canto II Becton&Dickinson).

Inhibition of Cell Adhesion to Vitronectin. The expression levels of $\alpha_V\beta_3$ and $\alpha_V\beta_5$ integrin receptors on WM266.4 cell lines were confirmed by flow cytometric analysis, as previously reported.[31] Next, the $\alpha_V\beta_3$ highly positive WM266.4 human melanoma cells were used for the inhibition of adhesion experiments. 96-well plates were coated overnight, at 4 °C, with VN (10 μg/mL) (V8379 Sigma). The plates were, then, washed with PBS solution and incubated at 37 °C for 1 h with PBS containing 1% bovine serum albumin (BSA). WM299.4 cells were centrifuged (RT, at 700*g*) in PBS, to remove serum, counted, and suspended in a serum-free medium at 7.0×10^5 cells/mL. Melanoma cell suspensions were preincubated with different amounts of the compounds, c(RGDyK)−GEM conjugates (final concentration ranged from 100 μM to 10 nM), at 37 °C for 30 min to allow the ligand−receptor equilibrium to be reached. Next, cells were plated on VN substrata (6 to 7 × 10^4 cells/well) and incubated at 37 °C for 1 h. The assays were conducted in the presence of 2 mmol/L $MnCl_2$. At the end of the incubation, the plates were washed with PBS to remove the nonadherent cells, and 200 μL of 0.5% crystal violet solution in 20% methanol was added. After 2 h of static incubation at 4 °C, the plates were examined at 540 nm in a counter-ELX800 system (Bio TEK Instruments). Experiments were done in triplicate and repeated at least three times. The values are expressed as % inhibition ± SEM of cell adhesion relative to cells exposed to vehicle alone (PBS).

Inhibition of Cell Invasion through Matrigel-Coated Filters by c(RGDyK)−GEM Conjugates. WM266.4 cells (0.2 × 10^6) were resuspended in their 24 h culture medium and then placed inside 12 mm, 8.0 μm pore, Millicell culture plate inserts (Millipore), coated with Matrigel (50 mg/filter; BD). Migration was allowed to occur in the presence or in the absence of different c(RGDyK)−GEM-conjugated compounds at 10 μM concentration each. At the end of the incubation (4 h at 37 °C in 10% CO_2-humidified atmosphere), the inserts were fixed in cold methanol and stained with DiffQuick solution. Cells on the upper surface of the filter were removed with a cotton swab. Migrated cells were counted by a light microscope (10×) in 10 random fields per well in separate experiments. Each treatment was performed at least in duplicate. The mean values of the migrated cells for each point were calculated from three independent experiments.[34]

Annexin V/PI Flow Cytometry Analysis. The percentages of apoptotic and necrotic cells were measured by flow cytometry using the annexin V/propidium iodide (PI) staining. The cells were exposed to conjugates **TC113** and **TC116** in comparison with GEM for 72 h treatment at a 1 μM dose. At the end of incubation, the cells were collected using Accutase cell detachment solution (Thermofisher), washed once with PBS, resuspended in 100 μL of 1× annexin-binding buffer at the concentration of 1 × 10^6 cells/mL, stained with 5 μL of annexin V FITC-conjugated (ImmunoTools, Friesoythe, Germany) and 1 μL of 100 μg/mL PI working solution. Cells were next incubated at 4 °C in dark condition for 15 min. At the end of the incubation, 400 μL of 1× annexin-binding buffer was added to each sample, and the cells were analyzed by flow cytometry (BD-FACS Canto). Cell populations with negative annexin V and PI signals were considered viable (Q3); cells with annexin V positive and PI negative signals were considered in early apoptosis (Q4); cells with annexin V and PI positive signals were considered in late apoptosis (Q2); and finally, cells with annexin V negative and PI positive signals were considered in necrosis (Q1). A minimum of 10 000 events were collected.

■ ASSOCIATED CONTENT

Ⓢ Supporting Information

The Supporting Information is available free of charge at https://pubs.acs.org/doi/10.1021/acs.jmedchem.1c01468.

Analytical data of the synthesized compounds (PDF)

■ AUTHOR INFORMATION

Corresponding Authors

Constantin Tamvakopoulos − *Center of Clinical Research, Experimental Surgery and Translational Research, Division of Pharmacology-Pharmacotechnology, Biomedical Research Foundation, Academy of Athens, Athens GR-11527, Greece;* ⓞ orcid.org/0000-0001-9627-4812; Phone: 210-6597475; Email: ctamvakop@bioacademy.gr

Vasiliki Sarli − *Department of Chemistry, Aristotle University of Thessaloniki, 54124 Thessaloniki, Greece;* ⓞ orcid.org/0000-0002-6128-8277; Phone: 2313997840; Email: sarli@chem.auth.gr

Authors

Theodora Chatzisideri − *Department of Chemistry, Aristotle University of Thessaloniki, 54124 Thessaloniki, Greece*

George Leonidis − *Department of Chemistry, Aristotle University of Thessaloniki, 54124 Thessaloniki, Greece*

Theodoros Karampelas − *Center of Clinical Research, Experimental Surgery and Translational Research, Division of Pharmacology-Pharmacotechnology, Biomedical Research Foundation, Academy of Athens, Athens GR-11527, Greece*

Eleni Skavatsou − *Center of Clinical Research, Experimental Surgery and Translational Research, Division of Pharmacology-Pharmacotechnology, Biomedical Research Foundation, Academy of Athens, Athens GR-11527, Greece*

Angeliki Velentza-Almpani − *Center of Clinical Research, Experimental Surgery and Translational Research, Division of Pharmacology-Pharmacotechnology, Biomedical Research Foundation, Academy of Athens, Athens GR-11527, Greece*

Francesca Bianchini − *Department of Experimental and Clinical Biomedical Sciences, University of Florence, 50134 Firenze, Italy*

Complete contact information is available at:
https://pubs.acs.org/10.1021/acs.jmedchem.1c01468

Notes

The authors declare no competing financial interest.

■ ABBREVIATIONS

ACN, acetonitrile; BOC, *tert*-butyloxycarbonyl; DCM, dichloromethane; cRGDyK, (cyclo Arg−Gly−Asp−D-Tyr−Lys); DIPEA, diisopropylethylamine; DMEM, Dulbecco's modified Eagle's medium; DMF, dimethylformamide; DMSO, dimethyl sulfoxide; 5-FU, 5-fluorouracil; GEM, gemcitabine; hCNT, human concentrative nucleoside transporter; NT, nucleoside transporter protein; PBS, phosphate-buffered saline; Py, pyridine; RGD, arginine−glycine−aspartic acid; TBSCl, *tert*-butyldimethylsilyl chloride; TFA, trifluoroacetic acid

■ REFERENCES

(1) Pauwels, B.; Korst, A. E. C.; Lardon, F.; Vermorken, J. B. Combined modality therapy of gemcitabine and radiation. *Oncologist* **2005**, *10*, 34−51.

(2) Kokkali, S.; Tripodaki, E. S.; Drizou, M.; Stefanou, D.; Magou, E.; Zylis, D.; Kapiris, M.; Nasi, D.; Georganta, C.; Ardavanis, A. Biweekly Gemcitabine/Nab-Paclitaxel as First-line Treatment for Advanced Pancreatic Cancer. *In Vivo* **2018**, *32*, 653−657.

(3) Lorusso, D.; Ferrandina, G.; Fruscella, E.; Marini, L.; Adamo, V.; Scambia, G. Gemcitabine in epithelial ovarian cancer treatment: current role and future perspectives. *Int. J. Gynecol. Cancer* **2005**, *15*, 1002−1013.

(4) Ai, D.; Guan, Y.; Liu, X. J.; Zhang, C. F.; Wang, P.; Liang, H. L.; Guo, Q. S. Clinical comparative investigation of efficacy and toxicity of cisplatin plus gemcitabine or plus Abraxane as first-line chemotherapy for stage III/IV non-small-cell lung cancer. *OncoTargets Ther.* **2016**, *9*, 5693−5698.

(5) Maréchal, R.; Mackey, J. R.; Lai, R.; Demetter, P.; Peeters, M.; Polus, M.; Cass, C. E.; Young, J.; Salmon, I.; Devière, J.; Van Laethem, J. L. Human equilibrative nucleoside transporter 1 and human concentrative nucleoside transporter 3 predict survival after adjuvant gemcitabine therapy in resected pancreatic adenocarcinoma. *Clin. Cancer Res.* **2009**, *15*, 2913.

(6) Plunkett, W.; Huang, P.; Xu, Y. Z.; Heinemann, V.; Grunewald, R.; Gandhi, V. Gemcitabine: metabolism, mechanisms of action, and self-potentiation. *Semin. Oncol.* **1995**, *22*, 3−10.

(7) Tonato, M.; Mosconi, A. M.; Martin, C. Safety profile of gemcitabine. *Anticancer Drugs* **1995**, *6*, 27−32.

(8) Giovannetti, E.; Laan, A. C.; Vasile, E.; Tibaldi, C.; Nannizzi, S.; Ricciardi, S.; Falcone, A.; Danesi, R.; Peters, G. J. Correlation between cytidine deaminase genotype and gemcitabine deamination in blood samples. *Nucleosides, Nucleotides Nucleic Acids* **2008**, *27*, 720−725.

(9) Moysan, E.; Bastiat, G.; Benoit, J.-P. Gemcitabine versus Modified Gemcitabine: a review of several promising chemical modifications. *Mol. Pharm.* **2013**, *10*, 430−444.
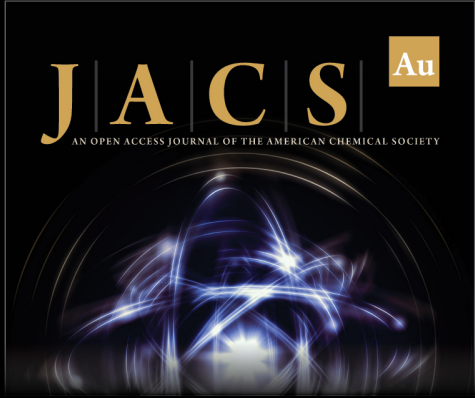
(10) Hynes, R. O. Integrins: bidirectional, allosteric signaling machines in their roles as major adhesion receptors. *Cell* **2002**, *110*, 673−687.

(11) Hynes, R. Integrins: a family of cell surface receptors. *Cell* **1987**, *48*, 549−554.

(12) Lino, R. L. B.; Dos Santos, P. K.; Pisani, G. F. D.; Altei, W. F.; Cominetti, M. R.; Selistre-de-Araújo, H. S. Alphavbeta3 integrin blocking inhibits apoptosis and induces autophagy in murine breast tumor cells. *Biochim. Biophys. Acta, Mol. Cell Res.* **2019**, *1866*, 118536.

(13) Katsamakas, S.; Chatzisideri, T.; Thysiadis, S.; Sarli, V. RGD-mediated delivery of small-molecule drugs. *Future Med. Chem.* **2017**, *9*, 579−604.

(14) Chatzisideri, T.; Leonidis, G.; Sarli, V. Cancer-targeted delivery systems based on peptides. *Future Med. Chem.* **2018**, *10*, 2201−2226.

(15) Ji, S.; Xu, J.; Zhang, B.; Yao, W.; Xu, W.; Wu, W.; Xu, Y.; Wang, H.; Ni, Q.; Hou, H.; Yu, X. RGD-conjugated albumin nanoparticles as a novel delivery vehicle in pancreatic cancer therapy. *Cancer Biol. Ther.* **2012**, *13*, 206−215.

(16) Zhang, J.; Zhang, P.; Zou, Q.; Li, X.; Fu, J.; Luo, Y.; Liang, X.; Jin, Y. Co-Delivery of Gemcitabine and Paclitaxel in cRGD-Modified Long Circulating Nanoparticles with Asymmetric Lipid Layers for Breast Cancer Treatment. *Molecules* **2018**, *23*, 2906.

(17) Han, H.; Jin, Q.; Wang, Y.; Chen, Y.; Ji, J. The rational design of a gemcitabine prodrug with AIE-based intracellular light-up characteristics for selective suppression of pancreatic cancer cells. *Chem. Commun.* **2015**, *51*, 17435−17438.

(18) Cox, N.; Kintzing, J. R.; Smith, M.; Grant, G. A.; Cochran, J. R. Integrin-Targeting Knottin Peptide-Drug Conjugates Are Potent Inhibitors of Tumor Cell Proliferation. *Angew. Chem., Int. Ed. Engl.* **2016**, *55*, 9894−9897.

(19) Chatzisideri, T.; Dalezis, P.; Leonidis, G.; Bousis, S.; Trafalis, D.; Bianchini, F.; Sarli, V. Synthesis and biological studies of c(RGDyK) conjugates of cucurbitacins. *Future Med. Chem.* **2021**, *13*, 877−895.

(20) Chatzisideri, T.; Thysiadis, S.; Katsamakas, S.; Dalezis, P.; Sigala, I.; Lazarides, T.; Nikolakaki, E.; Trafalis, D.; Gederaas, O. A.; Lindgren, M.; Sarli, V. Synthesis and biological evaluation of a Platinum(II)-c(RGDyK) conjugate for integrin-targeted photodynamic therapy. *Eur. J. Med. Chem.* **2017**, *141*, 221−231.

(21) Thysiadis, S.; Katsamakas, S.; Dalezis, P.; Chatzisideri, T.; Trafalis, D.; Sarli, V. Novel c(RGDyK)-based conjugates of POPAM and 5-fluorouracil for integrin-targeted cancer therapy. *Future Med. Chem.* **2017**, *9*, 2181−2196.

(22) Kapp, T. G.; Rechenmacher, F.; Neubauer, S.; Maltsev, O. V.; Cavalcanti-Adam, E. A.; Zarka, R.; Reuning, U.; Notni, J.; Wester, H.-J.; Mas-Moruno, C.; Spatz, J.; Geiger, B.; Kessler, H. A Comprehensive Evaluation of the Activity and Selectivity Profile of Ligands for RGD-binding Integrins. *Sci. Rep.* **2017**, *7*, 39805.

(23) Caccavari, F.; Valdembri, D.; Sandri, C.; Bussolino, F.; Serini, G. Integrin signaling and lung cancer. *Cell Adhes. Migr.* **2010**, *4*, 124−129.

(24) Kuphal, S.; Bauer, R.; Bosserhoff, A.-K. Integrin signaling in malignant melanoma. *Cancer Metastasis Rev.* **2005**, *24*, 195−222.

(25) Velu, P. P.; Cao, C.; Yan, T. D. Current surgical management of melanoma metastases to the lung. *J. Thorac. Dis.* **2013**, *5*, S274−S276.

(26) Guo, Z.-w.; Gallo, J. M. Selective Protection of 2′,2′-Difluorodeoxycytidine (Gemcitabine). *J. Org. Chem.* **1999**, *64*, 8319−8322.

(27) Zadlo, A.; Koszelewski, D.; Borys, F.; Ostaszewski, R. Mixed carbonates as useful substrates for a fluorogenic assay for lipases and esterases. *ChemBioChem* **2015**, *16*, 677−682.

(28) Singh, A.; Gao, M.; Beck, M. W. Human carboxylesterases and fluorescent probes to image their activity in live cells. *RSC Med. Chem.* **2021**, *12*, 1142−1153.

(29) Geisow, M. J.; Evans, W. H. pH in the endosome: Measurements during pinocytosis and receptor-mediated endocytosis. *Exp. Cell Res.* **1984**, *150*, 36−46.

(30) Geisow, M. J. Fluorescein conjugates as indicators of subcellular pH: A critical evaluation. *Exp. Cell Res.* **1984**, *150*, 29−35.

(31) Bianchini, F.; Portioli, E.; Ferlenghi, F.; Vacondio, F.; Andreucci, E.; Biagioni, A.; Ruzzolini, J.; Peppicelli, S.; Lulli, M.; Calorini, L.; Battistini, L.; Zanardi, F.; Sartori, A. Cell-targeted c(AmpRGD)-sunitinib molecular conjugates impair tumor growth of melanoma. *Cancer Lett.* **2019**, *446*, 25−37.

(32) Hofmann, U. B.; Westphal, J. R.; Van Muijen, G. N. P.; Ruiter, D. J. Matrix metalloproteinases in human melanoma. *J. Invest. Dermatol.* **2000**, *115*, 337−344.

(33) Hong, K.-H.; Kim, D. I.; Kwon, H.; Kim, H.-J. A fluoresceinylcarbonate-based fluorescent probe for the sensitive detection of biothiols in a HEPES buffer and its cellular expression. *RSC Adv.* **2014**, *4*, 978−982.

(34) Bianchini, F.; Giannoni, E.; Serni, S.; Chiarugi, P.; Calorini, L. 22: 6n-3 DHA inhibits differentiation of prostate fibroblasts into myofibroblasts and tumorigenesis. *Br. J. Nutr.* **2012**, *108*, 2129−2137.